



MONTCLAIR STATE
UNIVERSITY

Montclair State University
**Montclair State University Digital
Commons**

Theses, Dissertations and Culminating Projects

1-2022

Assessment of Digital Imaging Flow Cytometry in its Application of Harmful Algal Blooms Monitoring

Melissa Mazzaro
Montclair State University

Follow this and additional works at: <https://digitalcommons.montclair.edu/etd>



Part of the [Biology Commons](#)

Recommended Citation

Mazzaro, Melissa, "Assessment of Digital Imaging Flow Cytometry in its Application of Harmful Algal Blooms Monitoring" (2022). *Theses, Dissertations and Culminating Projects*. 870.
<https://digitalcommons.montclair.edu/etd/870>

This Thesis is brought to you for free and open access by Montclair State University Digital Commons. It has been accepted for inclusion in Theses, Dissertations and Culminating Projects by an authorized administrator of Montclair State University Digital Commons. For more information, please contact digitalcommons@montclair.edu.

Abstract

As harmful algal blooms (HABs) are becoming an increasing global threat to the health of people, animals, and aquatic ecosystems, finding ways to efficiently detect and manage blooms is critical. Traditional methods of identifying and enumerating phytoplankton cells involve light microscopy; however, this is a time-consuming and labor-intensive process. Meanwhile, digital imaging flow cytometry is a relatively novel and rapid method of enumerating and identifying particles within phytoplankton samples. Previous studies have documented comparable digital flow cytometry results to microscopy results; however, there are concerns relating to the underestimation of cells and misidentification of particles with their automated classification systems. Before digital imaging flow cytometry can be implemented into HAB monitoring protocols, a complete, thorough, and systematic comparison to light microscopy is needed using freshwater samples with a wide temporal and spatial range. This study investigates the accuracy and discrepancy of collected phytoplankton community data obtained by digital imaging flow cytometry and by light microscopy methods. The results demonstrate that microscopy cell densities ($p < 0.001$) and natural unit densities ($p < 0.001$) for both phytoplankton and cyanobacteria were significantly higher than the results obtained by the digital imaging flow cytometry methods. Additionally, taxa richness varied between the two methods, with the microscopy detecting significantly more phytoplankton taxa than digital imaging flow cytometry ($p = 0.016$). While digital imaging flow cytometry methods have potential in accurately enumerating and identifying phytoplankton, the findings of this study demonstrate that improvements to the digital imaging flow cytometry are needed before this method can be applied to routine HAB monitoring protocols.

MONTCLAIR STATE UNIVERSITY

Assessment of Digital Imaging Flow Cytometry in its Application of Harmful Algal Blooms

Monitoring

by

Melissa Mazzaro

A Master's Thesis Submitted to the Faculty of

Montclair State University

In Partial Fulfillment of the Requirements

For the Degree of

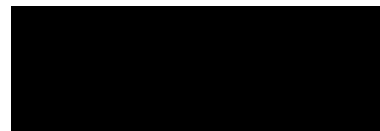
Master of Science

January 2022

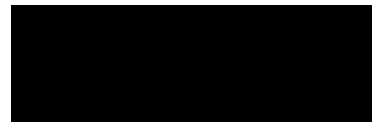
College of Science and Mathematics

Department of Biology

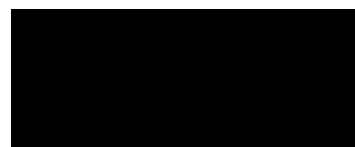
Thesis Committee:



Dr. Meiyin Wu, Thesis Sponsor



Dr. Lee Lee, Committee Member



Dr. Matthew Schuler, Committee Member

Assessment of Digital Imaging Flow Cytometry in its Application of Harmful Algal Blooms
Monitoring

A Thesis

Submitted in partial fulfillment of the requirements
For the degree of Master of Science

by
Melissa Mazzaro
Montclair State University
Montclair, NJ
2022

Acknowledgements

First, I would like to thank my thesis advisor, Dr. Meiyin Wu, for welcoming me into her lab back in 2017. At the time, I was an undergraduate student working on a study for my bachelor's degree. I have learned an incredible amount from her and her team at the New Jersey Center for Water Science and Technology since then. Thank you to her and the members of the lab for being so helpful, knowledgeable, and for giving me the opportunity to pursue my research. I would like to give a special thanks to lab members Kyle Clonan, Molly Hillenbrand, and Annie Hurley, who have assisted with field and data collection for this project. I'm very grateful to work with and learn from such a wonderful team.

I would also like to thank my committee members Dr. Lee Lee and Dr. Matthew Schuler. Dr. Lee, thank you for being so approachable and welcoming in your classrooms, and for teaching me so much about the field of microbiology. It has been a pleasure to have been one of your students. Dr. Schuler, thank you for assistance with statistical questions and for your insight on this project. It's been a pleasure to have your mentorship, to have been one of your students, and to have worked alongside you as your Graduate Assistant for Principles of Biology II. Thank you both for all the knowledge you two have given me since I started my master's degree at Montclair State University.

Thank you to the New Jersey Water Supply Authority (NJWSA), the United States Geological Survey (USGS), New Jersey Department of Environmental Protection (NJDEP), and the National Science Foundation (NSF) for the financial support and helping make this project possible.

Lastly, I would like to thank my family and friends; I would not have been able to make it this far without them. To my family, thank you for your endless love and support throughout my academic career. To my friends, those who I've met both at and outside of Montclair State University, thank you for all the advice and encouragement. Thank you, Michael Newman, for all your encouragement and support during the data analyzing and writing process. I appreciate all of you dearly.

Table of Contents

Abstract	1
Acknowledgements	4
List of Figures	6
List of Tables	8
1. Introduction	10
2. Methods	13
2.1 Phytoplankton Sample Information	13
2.2 Phytoplankton Identification	14
2.3.1 Cytometry	14
2.3.2 Cytometry Cell Enumeration	15
2.4 Microscopy Cell Enumeration	16
2.5 Statistical Analysis	16
3. Results	17
3.1 Microscopy Cell Densities, Natural Unit Densities, and Taxa Richness	17
3.2 Comparison of Data Obtained via Microscopy and Cytometry	18
3.3 Cytometry: Cell Enumeration Using Two Attributes	20
4. Discussion	21
4.1 Comparison between Cytometry and Microscopy	21
4.2 Comparison between Two Cytometry Attributes	24
5. Conclusion	26
References	47

List of Figures

- Figure 1:** An image of a *Dolichospermum* filament captured by the digital imaging flow cytometer. 27
- Figure 2:** Locations of the eight study sites located within the Raritan River Watershed, New Jersey. 28
- Figure 3:** Boxplot showing overall phytoplankton densities (cells/mL) obtained by the microscopy and digital imaging flow cytometry (cytometry) methods, plotted on a logarithmic scale. 29
- Figure 4:** Boxplot showing overall cyanobacteria cell densities (cells/mL) obtained by the microscopy and digital imaging flow cytometry (cytometry) methods, plotted on a logarithmic scale. 30
- Figure 5:** Boxplot showing overall phytoplankton natural unit densities (NU/mL) obtained by the microscopy and digital imaging flow cytometry (cytometry) methods, plotted on a logarithmic scale. 31
- Figure 6:** Boxplot showing overall cyanobacteria natural unit densities (NU/mL) obtained by the microscopy and digital imaging flow cytometry methods (cytometry), plotted on a logarithmic scale. 32
- Figure 7:** Boxplot showing overall phytoplankton taxa richness obtained by the microscopy and digital imaging flow cytometry (cytometry) methods. 33
- Figure 8:** Boxplot showing overall cyanobacteria taxa richness obtained by the microscopy and digital imaging flow cytometry methods (cytometry). 34
- Figure 9:** Boxplot showing the overall phytoplankton cell densities (cells/mL) obtained by the digital imaging flow cytometry's AP and VP attributes, plotted on a logarithmic scale. 35

Figure 10: Boxplot showing the overall cyanobacteria cell densities (cells/mL) obtained by the digital imaging flow cytometry's AP and VP attributes, plotted on a logarithmic scale. 36

Figure 11. Images of *Aphanothece* and images of *Aphanocapsa*. (a): a compound light microscope image of an *Aphanothece* colony taken under 400X total magnification, displaying its rod-shaped cells that are similar to *Aphanocapsa*. Scale bar is 10 μm ; (b): a compound light microscope image of an *Aphanocapsa* colony, taken under 400X total magnification. Scale bar is 10 μm ; (c): an image of an *Aphanocapsa* colony taken with the digital imaging flow cytometer, where the low image resolution makes *Aphanocapsa*'s cells less distinguishable. Photo credits: New Jersey Center for Water Science and Technology, Montclair State University. 37

List of Tables

Table 1: Location Information of the eight study sites located within the Raritan River Watershed, New Jersey.	38
Table 2: Minimum, maximum, and median phytoplankton* densities (cells/ml) obtained from the microscopy and digital imaging flow cytometry method, along with the results of the pairwise comparison analysis.	39
Table 3: Minimum, maximum, and median cyanobacteria densities (cells/ml) obtained from the microscopy digital imaging flow cytometry method, along with the results of the pairwise comparison analysis.	40
Table 4: The minimum, maximum, and median phytoplankton* natural unit densities (NU/ml) obtained from the microscopy and digital imaging flow cytometry methods, along with the results of the pairwise comparison analysis.	41
Table 5: The minimum, maximum, and median cyanobacteria natural unit densities (NU/ml) obtained from the microscopy and digital imaging flow cytometry methods, along with the results of the pairwise comparison analysis.	42
Table 6: Minimum, maximum, and median phytoplankton* taxa richness obtained from microscopy and digital imaging flow cytometry, along with the results of the pairwise comparison analysis.	43
Table 7: Minimum, maximum, and median cyanobacteria taxa richness obtained from microscopy and digital imaging flow cytometry, along with the results of the pairwise comparison analysis.	44

Table 8: The minimum, maximum, and median phytoplankton* cell densities (cells/ml) obtained by the digital imaging flow cytometry's AP and VP attributes, along with the results of the pairwise comparison analysis. 45

Table 9: The minimum, maximum, and median cyanobacteria cell densities (cells/ml) obtained by the digital imaging flow cytometry's AP and VP attributes, along with the results of the pairwise comparison analysis. 46

1. Introduction

Cyanobacteria are a group of photosynthetic prokaryotes that can be found in nearly any environment on Earth, including desert soils (Wehr et.al, 2015). In aquatic ecosystems, they can be found in the benthic region or free-floating in the water column with other types of phytoplankton, such as green algae (Wehr et.al, 2015; Chorus & Welker, 2021). They can also be found attached to other organisms, such as plants, or attached to submerged objects, such as rocks (Chorus & Welker, 2021). This study focuses on the cyanobacteria that are included in the phytoplankton group.

Within aquatic ecosystems, certain conditions such as nutrient-rich, stagnant or slow-moving water can cause the rapid growth of cyanobacteria, forming blooms in the waterbody. Other environmental conditions, including increased water temperatures and sunlight, can also cause cyanobacterial blooms. These blooms are referred to as Harmful Algal Blooms (HABs) due to the toxin-producing characteristic of some bloom-forming cyanobacteria. Toxins produced by cyanobacteria, known as cyanotoxins, have been reported to have harmful and deadly effects on humans, domestic animals, and both aquatic and terrestrial wildlife (Cox et al. 2003; Ferrão-Filho and Kozlowsky-Suzuki 2011; Metcalf and Codd, 2012). HABs can also negatively impact aquatic ecosystems by altering the water chemistry, such as reducing dissolved oxygen levels (Griffith and Gobler, 2020). When a HAB forms, turbidity is increased in the waterbody, which can prevent sunlight from reaching submerged plants and thus inhibit them from photosynthesizing (Kidwell, 2015). Dissolved oxygen levels are further reduced when the cyanobacteria decompose, as this process requires oxygen (Cui et al., 2021). This great reduction in dissolved oxygen levels can lead to hypoxic or anoxic conditions in the waterbody, where oxygen levels are too low to support aquatic organisms (Cui et al., 2021). For example,

deoxygenation from HABs have contributed to numerous fish kill incidents (Rabalais et. al, 2002; Piontkovski et. al, 2012; Kidwell, 2015).

The presence of HABs has increased globally since the 1980s; a trend that is expected to continue due to climate change (Griffith and Gobler, 2020; Ho et. al, 2019; Chapra et. al, 2017; Carey et. al, 2021). Climate change will promote conditions associated with HAB growth, such as warmer water temperatures for longer durations and nutrient loading from more intense and frequent storm events (Griffith and Gobler, 2020). Periods of drought will also alter hydrologic conditions by reducing water flow, causing stagnant or slow-moving water (Carey et. al 2012). Since HABs are a threat to the health of humans, animals, and aquatic ecosystems, efficient, sufficient, and accurate monitoring and management of these blooms is imperative.

Monitoring HABs includes measures such as determining the cell density or natural unit density of the bloom and identifying the types of phytoplankton that are present. These actions are needed as some federal and state environmental agencies have safety guidelines for HAB regulation based on cell and/or natural unit densities. For example, the New Jersey Department of Environmental Protection will advise the public against recreational use of the waterbody when cyanobacteria cell counts are greater than 80,000 cells/ml, or if the level of cyanotoxins exceeds the established public health standards, due to the risk of negative health effects HABs pose (NJDEP, 2021). Identifying the types of phytoplankton present allows for accurate enumeration of cyanobacteria, an understanding of the phytoplankton community composition, and the detection of any potentially toxin-producing cyanobacteria in the HAB. Traditionally, light microscopy is used when enumerating and identifying phytoplankton cells. However, this method is time-consuming and labor-intensive, which are non-ideal circumstances for early detection and rapid response of a suspicious HAB event.

Digital imaging flow cytometry (referred to as cytometry in this study) techniques combine features of flow cytometry and microscopy to process phytoplankton samples. These automated systems have imaging capabilities and data-processing algorithms that allow for the classification of small particles, such as phytoplankton (**Figure 1**) (Fluid Imaging Technologies, 2017). Enumeration of phytoplankton natural units and the measurement of morphological attributes, such as area and volume, are calculated through a particle analyzing software that is utilized by the cytometer (Yokogawa Fluid Imaging Technologies, 2018). Thus, cytometers can gather more information than microscopy techniques with little human involvement. Archived images and particle information also allow for the data to be reanalyzed when needed. Another benefit of this method is the ability to process more samples at a faster rate than microscopy techniques. This rapid processing time eliminates the need for preservatives, such as Lugol's solution.

There are several cytometers currently on the market, including the FlowCam (Yokogawa Fluid Imaging Technologies), the Imaging FlowCytobot (McLane Research Laboratories), the Accuri C6 Flow Cytometer (Becton and Dickinson Biosciences), and the CytoBuoy (CytoBuoy b.v.). However, the accuracy of the data obtained by cytometry methods is still under investigation (Alvarez et. al, 2014). For example, using the area of a particle to calculate cell abundance is currently recommended by a cytometry manufacturer (Yokogawa Fluid Imaging Technologies n.d; Lehman et al. 2017). However, in the images of large or dense colonies, cells tend to overlap and therefore, their area and abundance can be underestimated (Yokogawa Fluid Imaging Technologies, n.d). Calculating cell density using the volume of a particle may be a more precise method, since it considers the three-dimensional shape of colonial taxa.

The benefits and limitations of cytometry need to be compared to microscopy methods to fully assess its capabilities for HAB monitoring. Thus, the objective of this study is to evaluate the application of cytometry in HAB monitoring. This study evaluates cytometry's performance in monitoring phytoplankton by comparing the results with microscopy data. Further investigation of measuring cell density using different particle attributes (area vs. volume) obtained by a cytometry method was also conducted. The same, natural water samples were analyzed by both methods, but cell enumeration strategy followed the method's own specific protocol with a goal to illustrate the strengths and weaknesses of cytometry in its applications towards HAB monitoring.

2. Methods

2.1 Phytoplankton Sample Information

From August 2020 to January 2021, 10 freshwater samples were collected from 8 sites in the Raritan River Watershed in New Jersey, for a total of 80 samples (**Figure 2** and **Table 1**). Samples were collected in 500ml amber plastic bottles, kept on ice, and were transported to a Montclair State University laboratory for processing. Fresh samples were processed through the cytometer upon returning to the laboratory. After the fresh samples were taken for cytometer analysis, the samples were preserved with 0.5% Glutaraldehyde and kept in the dark at 4°C until the light microscopy analysis. For all samples, three replicates were conducted under both methods and cell density, natural unit density, and taxa richness for phytoplankton, including cyanobacteria, were recorded.

2.2 Phytoplankton Identification

For both methods, visual inspection was used to identify and count the phytoplankton observed. Phytoplankton were identified to genus level whenever possible using published identification guides including *Freshwater algae of North America: ecology and classification* (Wehr et.al, 2015), *Cyanoprokaryota-1. Teil/Part 1: Chroococcales* (Komárek & Anagnostidis 2008), *Cyanoprokaryota-2. Teil/Part 2: Oscillatoriales* (Komárek & Anagnostidis 2008), and *Cyanoprokaryota-3. Teil/Part 3: Heterocytous Genera* (Komárek, 2013).

2.3.1 Cytometry

A digital imaging flow cytometer (FlowCam Cyano, Yokogawa Fluid Imaging Technology, Inc. Scarborough, Maine) was selected for this study. This automated technique uses a combination of flow cytometry, microscopy, and fluorescence detection to image, analyze, and enumerate particles of interest in a sample (Fluid Imaging Technologies, 2017). Fresh samples were inverted 25 times before pipetting 250 μl into a 96 well plate. The 96 well plate was then placed into the cytometer's Automated Liquid-Handling System, where mechanical and computational robotics are used to pipet samples into the sample inlet port. Once a replicate had been processed through the cytometer, the flow cell was washed with 100 μl of 1% Contrad Soap solution and rinsed with 900 μl of deionized water. Since most phytoplankton are between 2 to 200 μm , a 10X objective lens (100X magnification) paired with a flow cell of 80 μm in depth x 700 μm in width was used when processing samples (Mullin, 2001). AutoImage mode, a setting where images are taken at a fixed rate, was selected for sample processing. Images taken were then analyzed and attributes such as color, shape, and texture were recorded for each particle through the cytometer's particle analysis software (VisualSpreadsheet v. 4.13.2).

2.3.2 Cytometry Cell Enumeration

For solitary phytoplankton, the particles per milliliter obtained from the particle analysis software was also regarded as that taxon's cell density in cells per milliliter. The particles per milliliter of each colonial and filamentous taxon were also regarded as natural unit density. The same particle analysis file was analyzed for both cytometry attributes used to calculate cell densities: area and volume. With the cytometer selected for this study, it is currently recommended by the manufacturer to use the area of a particle (AP) to determine cell density. To calculate phytoplankton cell density with the AP attribute, the particle analysis software assumes all particles are circular and utilizes the diameter of a particle to calculate its area (Yokogawa Fluid Imaging Technologies, 2020). The following procedure was used to determine cell density for colonial and filamentous taxa using AP. First, the average area of a single cell in a particle (colony or filament) was calculated. A selection of at least 4 images of the same taxon were collected from the sample's particle analysis file. The total area of the colonies or filaments was then calculated and used to determine the average area of 1 cell by dividing it with the number of cells manually counted in all selected images. After the average area of 1 cell had been determined, all images of this taxon were isolated in the particle analysis file. The particles per milliliter for this taxon was extracted from the particle analysis software, and a summary file of all selected images was exported to obtain the average area of all the selected particles. The average cell density for this taxon was then calculated by multiplying the particles per milliliter by the taxon's average particle area, and then dividing by the average area of 1 cell.

To calculate cell density for colonial and filamentous taxa using the volume of a particle (VP), the same procedure listed above was used; however, the total area, average cell area, and the average particle area in the steps above were replaced with the total volume, average cell

volume, and the average particle volume. The particle analysis software calculated volume by measuring the particle's thickness and length from the 2D image. These two measurements were then used to calculate the particle's volume, with the assumption that the particle is a sphere.

2.4 Microscopy Cell Enumeration

Microscopy cell enumeration was conducted using a compound light microscope (x Scientific, AX 800 Series) and a modified Palmer-Maloney counting chamber (PhycoTech, depth: 0.548 mm). Samples were inverted 25 times before 0.11 mL was taken for analysis. Under 400X magnification, cells were counted until 40 fields of views were observed. To determine cell density for each taxon, the total volume surveyed was first calculated by multiplying the number of fields of view surveyed by the volume of the field of view. After converting the total volume to milliliters, a conversion factor was computed to determine how many specimens of the same taxa would be present in 1 milliliter of the sample. The conversion factor was then multiplied by the average number of cells counted to determine cell density, in cells per milliliter. Natural unit density, in natural units per milliliter, was calculated for each taxon by multiplying the same conversion factor by the average number of natural units counted. Since natural units of phytoplankton under 2 μm cannot be detected with the cytometer used in this study, taxa with a natural unit size less than 2 μm were removed from the microscopy data in this study (Yokogawa Fluid Imaging Technologies, 2018).

2.5 Statistical Analysis

Statistical analyses were computed using non-parametric tests due to the lack of normality in the data collected, which was verified with a Shapiro-Wilk test. A pairwise comparison analysis using the Mann-Whitney U test was used to determine if there was a

significant difference between methods and cell densities, natural unit densities, and taxa richness detection. Sites were analyzed both independently and collectively. An $\alpha = 0.05$ was used to determine if there was a significant difference. All tests and the summarization of data were performed through RStudio (Version 1.2.5033).

3. Results

3.1 Microscopy Cell Densities, Natural Unit Densities, and Taxa Richness

In order to better compare the two methodologies, samples were collected from 8 study sites over three seasons (summer, fall, and winter) to include a diverse range of cell densities and community compositions in this analysis. The overall phytoplankton cell densities recorded by microscopy methods ranged from 310 to 1,085,728 cells/ml, where the minimum was found at site D and the maximum at site A (**Table 2**). Cyanobacteria cell densities also widely varied with an overall range of 0 to 1,074,641 cells/ml (**Table 3**). Out of the 8 sites, cyanobacteria were present in all samples from sites A, C, and F. In the remaining 5 sites, cyanobacteria were present in about 82% of the samples. Thus, the minimum cyanobacteria cell density was 0 cells/ml at sites B, D, E, G, and H (**Table 3**). The maximum cyanobacteria cell density was observed at site A (**Table 3**).

Overall phytoplankton natural unit densities obtained by the microscopy method had a range of 310 to 101,089 NU/ml, while 0 to 91,306 NU/ml was the overall range of cyanobacteria natural unit densities (**Table 4** and **Table 5**). The maximum phytoplankton and cyanobacteria natural unit densities were found at site A. Site D had the minimum phytoplankton natural unit density, while sites B, D, E, G, and H had the minimum cyanobacteria natural unit density.

A range of 2 to 31 phytoplankton taxa were found under the microscopy method; this maximum was found at site C, while site H had the minimum (**Table 6**). Total cyanobacteria taxa richness documented from this method ranged from 0 to 10 taxa (**Table 7**). Sites A and C had the maximum cyanobacteria taxa richness, and sites B, D, E, G, H had the minimum taxa richness of 0 (**Table 7**).

3.2 Comparison of Data Obtained via Microscopy and Cytometry

Phytoplankton cell densities calculated by the cytometry method were significantly different compared to the results obtained via the microscopy method ($p < 0.001$) (**Figure 3** and **Table 2**). The cytometry method calculated an overall phytoplankton cell density range of 16 to 44,378 cells/ml, where the minimum cell density was found at site F, and the maximum at site A (**Table 2**). Cyanobacteria cell densities calculated by the cytometry method were also significantly different compared to the results obtained via the microscopy method ($p < 0.001$) ranging from 0 to 42,791 cells/ml (**Figure 4** and **Table 3**). Contrasting to microscopy, cyanobacteria were present in all samples from 2 sites under the cytometry method: sites A and C. The maximum cyanobacteria cell density of 42,791 cells/ml was observed at site A (**Table 3**). In the remaining 6 sites, cyanobacteria were present in about 40% of the samples under the cytometry method (**Table 3**). Overall, the cytometry method resulted in substantially underestimated phytoplankton and cyanobacteria cell densities in comparison to the microscopy cell counts (**Figure 3** and **Figure 4**).

Overall, phytoplankton natural unit densities determined by the cytometry and microscopy methods were also significantly different ($p < 0.001$) (**Figure 5** and **Table 4**). In the cytometry method, the minimum phytoplankton natural unit density was 16 NU/ml at site F compared to 310 NU/ml observed under the microscope at site D (**Table 4**). Although the site

with the minimum phytoplankton natural unit density differed between microscopy and cytometry, the site identified with the maximum phytoplankton natural unit density, site A, was the same between the two methods. However, the cytometry method calculated a maximum phytoplankton density of 1,817 NU/ml compared to a much higher density of 101,089 NU/ml observed under the microscope (**Table 4**). Consistent with the observation of phytoplankton results, the overall cyanobacteria natural unit densities determined by both methods were significantly different as well ($p < 0.001$) (**Figure 6** and **Table 5**). The maximum cyanobacteria natural unit density was also found at site A using both methods, however, the cytometry method found a maximum of only 1,330 NU/ml compared to 91,306 NU/ml observed under the microscope (**Table 5**). Sites B, D, E, F, G, and H had the minimum cyanobacteria natural unit density of 0 NU/ml (**Table 5**). Consequently, just as the cytometry cell densities were significantly underestimated in comparison to the microscopy method, so were the natural unit densities (**Figure 5** and **Figure 6**).

A significant difference was found in the overall phytoplankton taxa richness recorded between the cytometry and microscopy methods ($p = 0.016$) (**Figure 7** and **Table 6**). Amongst the sites, differences in phytoplankton taxa richness were found at sites A ($p = 0.002$), B ($p = 0.012$), C ($p < 0.001$), F ($p = 0.001$), and G ($p = 0.003$) (**Table 6**). The minimum phytoplankton taxa richness, for the cytometry method, was 2 taxa in sites B and G (**Table 6**). For these two sites, a minimum of 4 phytoplankton taxa was recorded under the microscopy method (**Table 6**). Unlike the microscopy method, where a maximum of 31 phytoplankton taxa were observed, the cytometry method resulted in a maximum phytoplankton taxa richness at site A with 26 taxa (**Table 6**). The presence of certain taxa was also not consistent between a sample analyzed under both methods. For example, *Pediastrum*, a green alga, would be present in a sample under

cytometry analysis, but would not be detected in the same sample that was processed with microscopy. Thus, these two methods were inconsistent in taxa detection and the cytometry method was significantly underestimating phytoplankton taxa richness when a difference was found (**Table 6**).

Overall, a significant difference between cyanobacteria taxa richness obtained by the two methods was found ($p < 0.001$) (**Figure 8** and **Table 7**). A maximum of 9 cyanobacteria taxa were detected at site A under the cytometry method, whereas the microscopy method had a maximum of 10 taxa at sites A and C (**Table 7**). Sites B, D, E, F, G, and H had the minimum cyanobacteria taxa richness of 0 (**Table 7**). The cytometry method generally detected less cyanobacteria taxa than the microscopy method.

3.3 Cytometry: Cell Enumeration Using Two Attributes

Two cytometer attributes, AP and VP, were used to calculate cell densities. While the AP attribute is the manufacturer's recommendation for determining cell density, the VP attribute was also utilized for comparison purposes. Overall phytoplankton cell densities were found to be similar between these two attributes ($p = 0.917$) (**Figure 9** and **Table 8**). Both attributes found a minimum phytoplankton cell density of 16 cells/ml at site F (**Table 8**). Site A had the maximum cell density for both attributes, however, the VP attribute calculated a higher cell density of 53,135 cells/ml, whereas the AP attribute recorded 44,378 cells/ml (**Table 8**).

Overall cyanobacteria cell densities were also similar calculated using the AP and VP attributes ($p = 0.939$) (**Figure 10** and **Table 9**). Cyanobacteria were not always detected in samples from 6 of the 8 sites under the cytometry method, and thus, the attributes both had a minimum cell density of 0 cells/ml at sites B, D, E, F, G, and H (**Table 9**). Site A had the

maximum cyanobacteria cell density in both attributes; however, the AP attribute found a maximum of 51,393 cells/ml and the AP attribute found a lower maximum of 42,791 cells/ml (**Table 9**). Despite using different formulas to determine cell abundance, the AP and VP attributes produced statistically similar results.

4. Discussion

4.1 Comparison between Cytometry and Microscopy

Several previous studies (Alvarez et. al 2014, Buskey and Hyatt, 2006, Sieracki et al. 1998) have documented comparable results from cytometry methods to results obtained from microscopy. However, these studies primarily focus on unicellular taxa from laboratory cultures or marine environments. This study intentionally included a diverse range of freshwater samples with a wide temporal and spatial distributions in order to better examine the capacities of cytometry for HABs monitoring. The results from this study contradict these previous published findings; the phytoplankton and cyanobacteria cell and natural unit densities determined by the cytometry and microscopy methods were significantly different. Microscopy cell and natural unit densities were significantly higher than the densities obtained by the cytometry methods.

One study (Park et. al, 2019) investigated the use of these two methods to enumerate *Microcystis* colonies found that the cytometry method was underestimating cell counts and concluded that a correction factor was needed while using cytometry for cell enumeration. This is not only consistent with the results of this study, but it also highlights limitations in enumeration using cytometry. Despite utilizing various attributes, colonies and filamentous taxa are captured as 2D images under cytometry methods. All the cells in filamentous or colonial structures may not be visible in the same plane, thus creating errors while enumerating cells with the cytometry method. Here, microscopy methods have the advantage of being able to adjust

focal depth, allowing for better examination and enumeration of filamentous and colonial specimens. Using images for phytoplankton enumeration can also pose an issue if there are multiple specimens clustered in a frame. The particle analysis software will count the cluster as one particle and combine the area or volume of all specimens in an image, resulting in inaccurate counting and measurements. Thus, images with multiple specimens in a single frame must be omitted during the cytometer data review, further underestimating cell abundance.

Using cytometry 2D images for analysis may also pose limitations for identifying phytoplankton. The images obtained have a lower taxonomic resolution, which may make it difficult for identification to the targeted taxonomic level, preferably genus or species level. A blurry image may also make it difficult to accurately identify a specimen. Further, in natural water samples, detritus or non-phytoplankton images are frequently taken and must be omitted manually during the data review. Moreover, while a particle analysis software is capable of distinguishing cells of different morphological shapes automatically, taxa that are similar in shape and size are at risk of being mis-identified (Jin et. al, 2018; Buskey and Hyatt 2006). Though, using fluorescence detection, cell staining, and adjusting cytometry settings may improve identification (Jin et. al 2018; Camoying and Yñiguez, 2016), to obtain good quality data, a trained phytoplankton taxonomist should always review and examine images obtained from a cytometer as a part of the laboratory quality control process.

In this study, a significant difference in taxa richness was found between results obtained via the cytometry and microscopy methods. Despite processing a much smaller sample volume, microscopy analysis detected more phytoplankton and cyanobacteria taxa than the cytometry method. There were other inconsistencies as well, for example, site F was a location where cyanobacteria were not detected in all ten samples under the cytometry method, but

cyanobacteria were present in all microscopy observations. The adjustable focal level gives the microscopy method another advantage for identification, as it allows for a better observation of the specimen's taxonomic detail. With a higher taxonomic resolution, a more reliable identification to the genus or species level can be better accomplished. Additionally, the ability to change focal level allows for a wider size range of phytoplankton to be detected. Other microscopy features, such as phase contrast or fluorescence, can also be utilized to assist in the identification of phytoplankton and cyanobacteria.

A few taxa observed under the microscopy method were never detected in the cytometry method but were observed during microscopy analysis. For example, *Aphanothece*, *Raphidiopsis*, and *Planktolyngbya* are some cyanobacteria taxa that were not found using the cytometry method. *Planktolyngbya* and *Raphidiopsis* filaments are typically very thin, with *Planktolyngbya* ranging from 3 to 5 μm wide and *Raphidiopsis* ranging from 1 to 5 μm wide, which could cause them to either be misidentified or overlooked (Komárek & Anagnostidis 2008; Komárek, 2013). *Aphanothece* cells can range from 1 to 4 μm and closely resemble *Aphanocapsa* (Komárek & Anagnostidis 2008). The distinguishing feature of *Aphanothece* are their rod-shaped cells, however, due to their small size, it could be hard to distinguish this taxon from *Aphanocapsa*'s coccoid cells in cytometry images (**Figure 11**). Other phytoplankton, such as *Urosolenia* and *Nephroselmis* were also not detected in the cytometry samples. These phytoplankton represent taxa that have delicate features, such as fragile cell walls or distinct flagella, that could easily be missed in cytometry images with a lower resolution.

Both methods had reproducible cell densities, natural unit densities, and taxa richness within their replicates. However, results from this study demonstrate that there are significant differences between cytometry and microscopy results. There are trade-offs one must consider

when deciding to apply an enumeration and identification technique to their samples. One advantage of the cytometry method is that it eliminates the need for preservation, reducing the amount of chemical use, chemical waste, and labor. Moreover, the use of preservatives has been shown to alter the appearance of cells, which can influence identification or biomass estimations (Menden et. al, 2001; Hällfors et. al 1979). Operators can also use the permanent files created by the cytometer for future reference. Further, cytometry methods can process samples at a much faster rate than microscopy analysis, which is more ideal in HAB monitoring scenarios, enabling early detection and rapid response to a suspicious HAB incident.

This study shows that the cytometry method has potential to be an effective instrument for HAB monitoring and research. However, there are clear technical challenges that need to be addressed before this technique can be used for precise and reliable water quality analysis. As cytometry methods are relatively new in the industry, additional improvements are needed to optimize both its hardware and software to accurately assess HABs. The cytometry cameras should be enhanced for a higher resolution to improve the identification of phytoplankton. Improvements should also be applied to the particle analysis software to accurately count colonial and filamentous taxa, making this method more reliable. As these improvements within cytometry methods are made, the updated system should still be compared to traditional light microscopy to assess its capacity and performance.

4.2 Comparison between Two Cytometry Attributes

The current method for determining cell density via cytometry utilizes a particle's area, following the manufacturer's recommendation; however, this study's results have shown that large or dense colonies are under-counted due to cell overlap within its image (Yokogawa Fluid Imaging Technologies n.d; Lehman et al. 2017). Hence, the VP attribute was also applied when

calculating cell counts to determine if this attribute would improve the cell counts of colonial and filamentous taxa, as it would better account for their three-dimensional shape. This study demonstrates that phytoplankton and cyanobacteria cell densities from AP and VP attributes obtain similar results. However, when examining site-specific results, the VP cell densities were greater than AP cell densities when counting large/dense colonies, particularly while examining a suspicious HAB event.

A previous study (Hrycik et. al, 2019) investigated the biovolume differences obtained by FlowCam's AP and VP attributes and found that VP attribute had more accurate estimates than AP. Therefore, when employing cytometry for cell enumeration, using the VP attribute may be more reliable, as it considers the three-dimensional shape of cyanobacteria. Since the method of calculating cell density via cytometry are influenced by the morphology of phytoplankton, future research should work to improve the particle analysis software to accurately count colonial and filamentous phytoplankton. For example, the VP attribute still relies on the particle's length and thickness measurements from a 2D image. Moreover, the VP estimates assume that a particle is a sphere, which does not apply to polymorphic organisms such as phytoplankton. This misassumption can lead to miscalculations and underestimations. Additionally, the hardware and software should be improved to account for smaller phytoplankton while processing HAB samples. In this study, phytoplankton under 2 μm were omitted from the microscopy data because they were not visible with the cytometer used. Numerous cyanobacteria smaller than 2 μm , such as *Synechococcus*, are often abundant in temperate waterbodies and HABs (Olsen & Mahoney, 2001; Komárek & Anagnostidis, 2008; Liu et. al 2011). Therefore, not detecting phytoplankton under 2 μm further contributes to underestimations in cell density and taxa richness. In order to be a reliable method in HAB monitoring, cytometry methods should

advance their capabilities to analyze and detect an incredibly wide range of particle sizes and shapes.

5. Conclusion

As the frequency and intensity of HABs are expected to increase with climate change, efficient monitoring of suspicious HAB events is imperative to ensure public health safety. Cytometry methods have demonstrated their capabilities in rapidly obtaining massive amounts of particle information, making the method a promising candidate for HABs monitoring. If proven effective, the cytometry method would be more ideal, as light microscopy is time-consuming and labor-intensive. However, issues relating to identification and underestimation show that further hardware and software improvements are needed for cytometry to be more reliable. When deciding which method to use, one should consider sample processing time, taxonomic resolution, size range of target specimens, and the effects preservation may have on the specimens. Considerations should also be applied when calculating cell density with a cytometry method, as a correction factor may be required. While light microscopy is the traditional approach, advancements in cytometry research may have potential in the future of HAB monitoring.



Figure 1: An image of a *Dolichospermum* filament captured by the digital imaging flow cytometer.

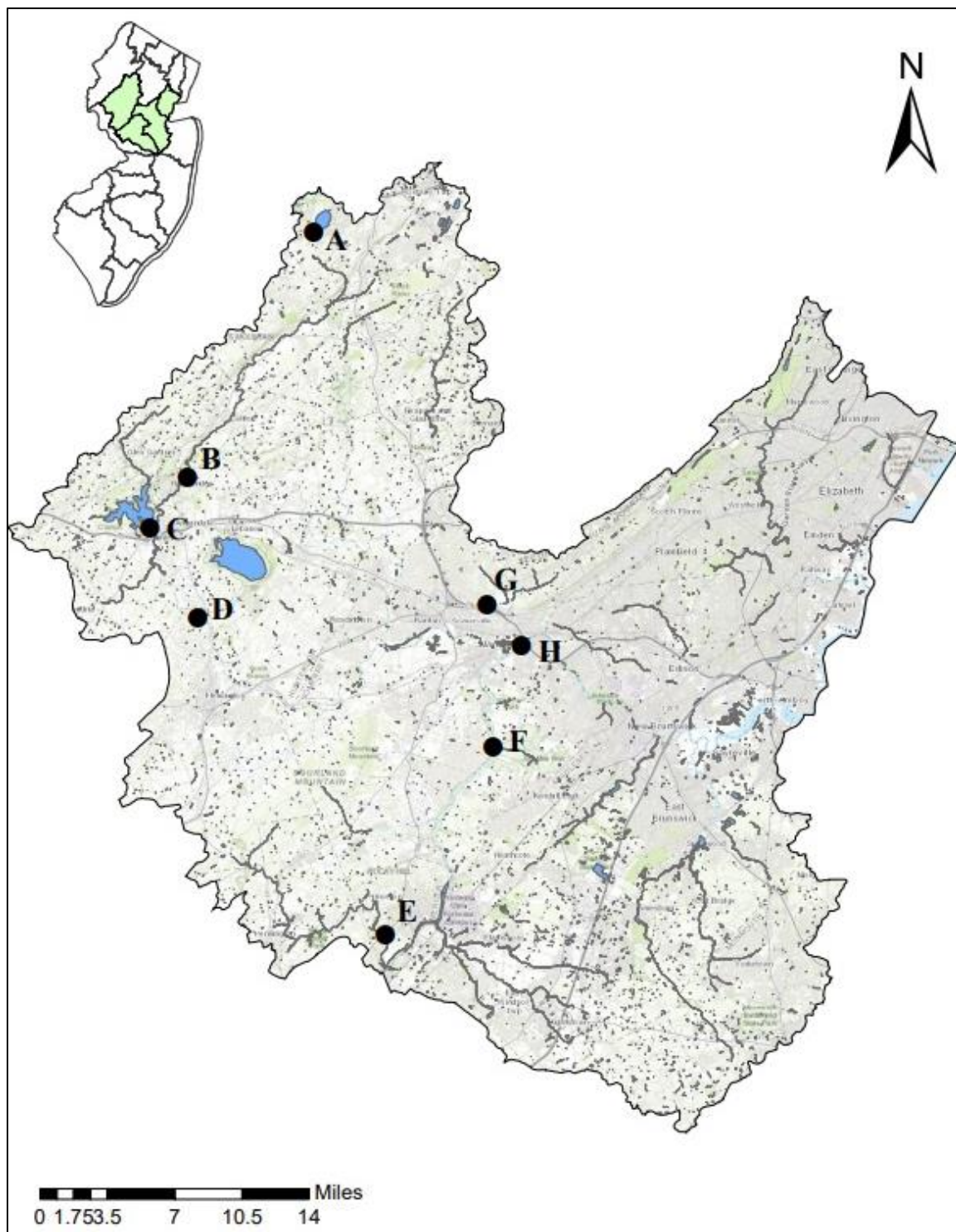


Figure 2: Locations of the eight study sites located within the Raritan River Watershed, New Jersey.

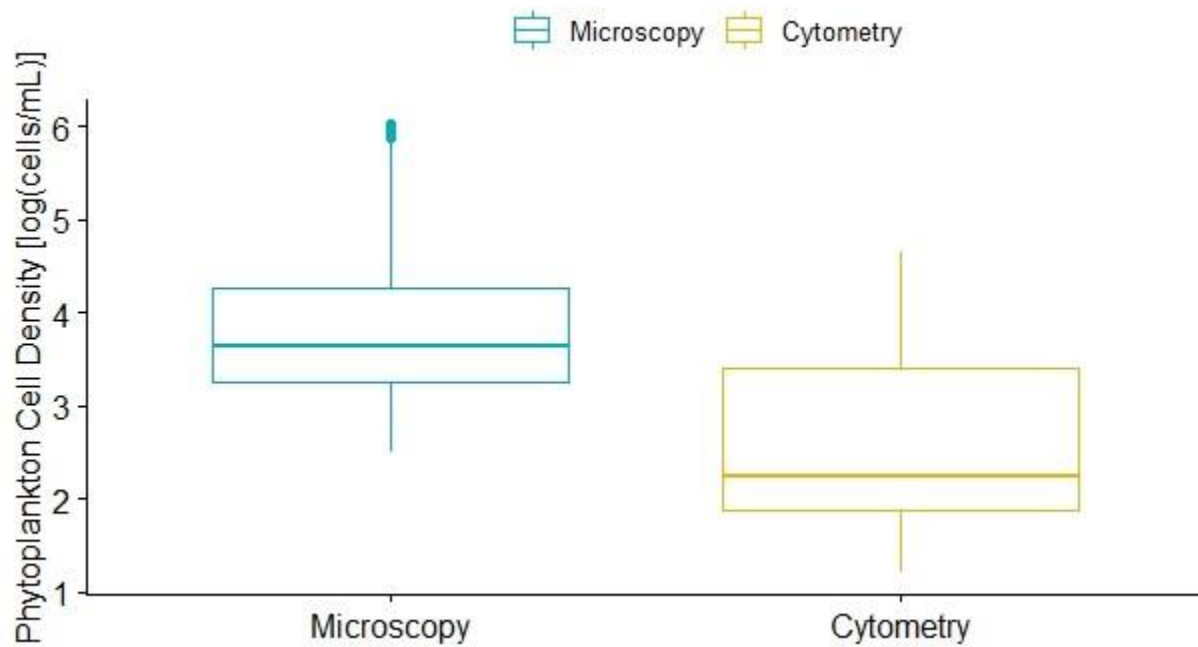


Figure 3: Boxplot showing overall phytoplankton densities (cells/mL) obtained by the microscopy and digital imaging flow cytometry (cytometry) methods, plotted on a logarithmic scale.

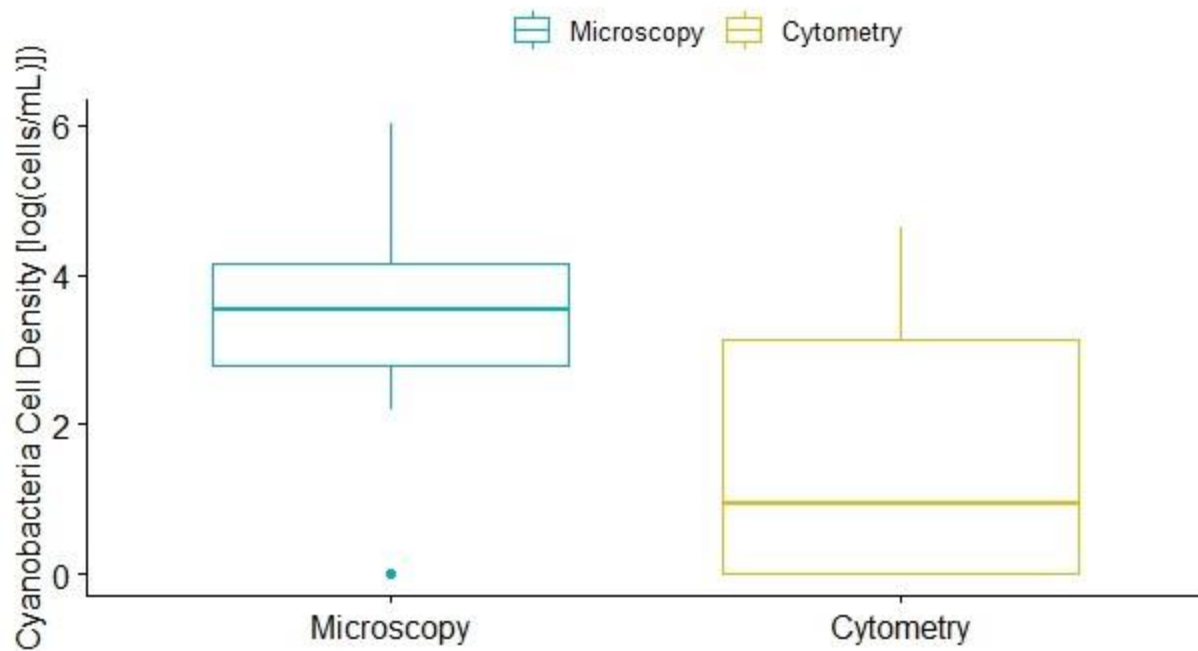


Figure 4: Boxplot showing overall cyanobacteria cell densities (cells/mL) obtained by the microscopy and digital imaging flow cytometry (cytometry) methods, plotted on a logarithmic scale.

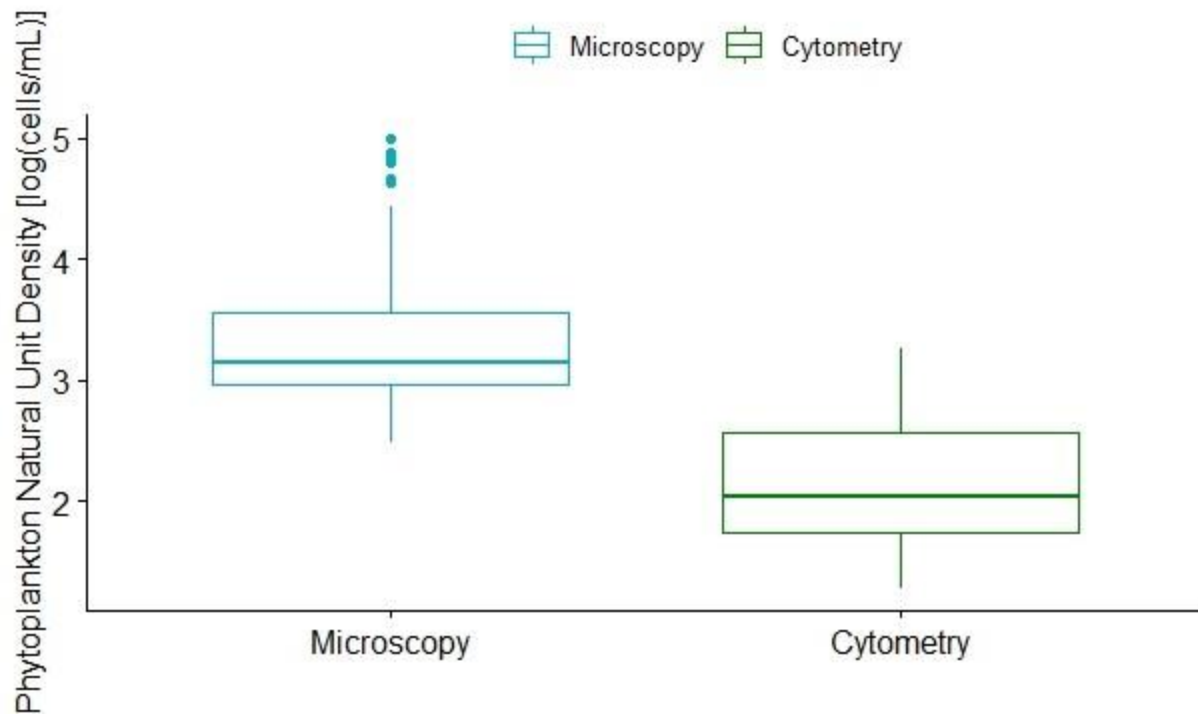


Figure 5: Boxplot showing overall phytoplankton natural unit densities (NU/mL) obtained by the microscopy and digital imaging flow cytometry (cytometry) methods, plotted on a logarithmic scale.

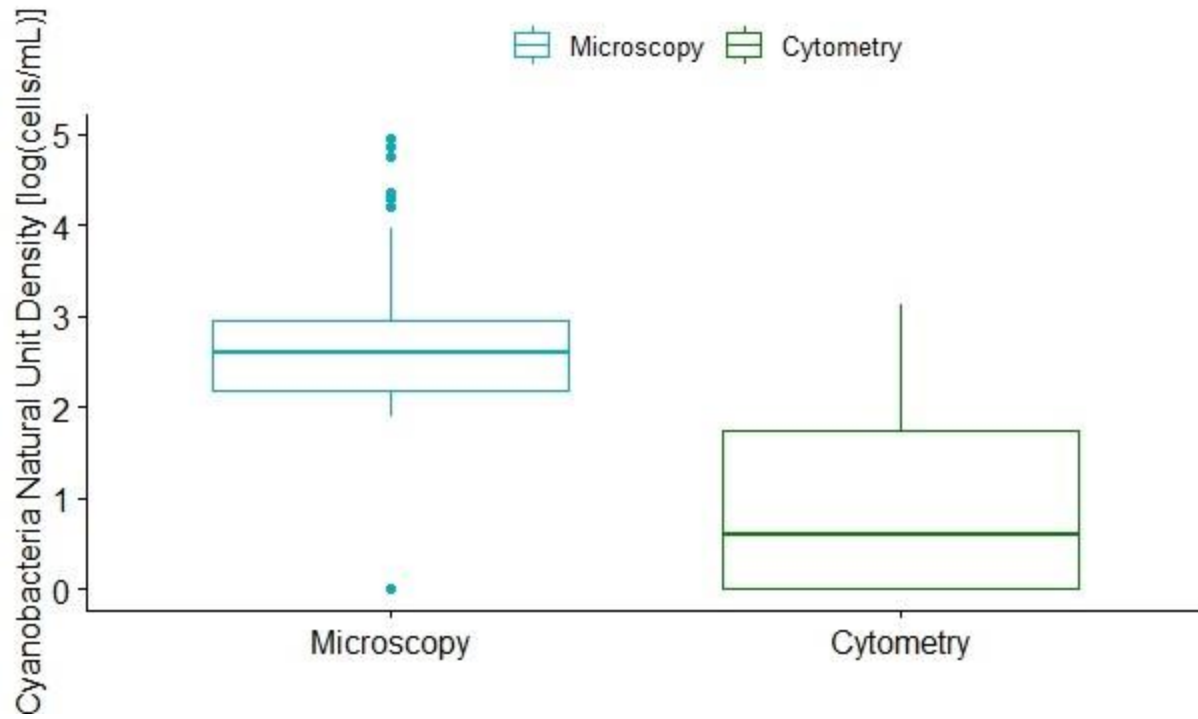


Figure 6: Boxplot showing overall cyanobacteria natural unit densities (NU/mL) obtained by the microscopy and digital imaging flow cytometry methods (cytometry), plotted on a logarithmic scale.

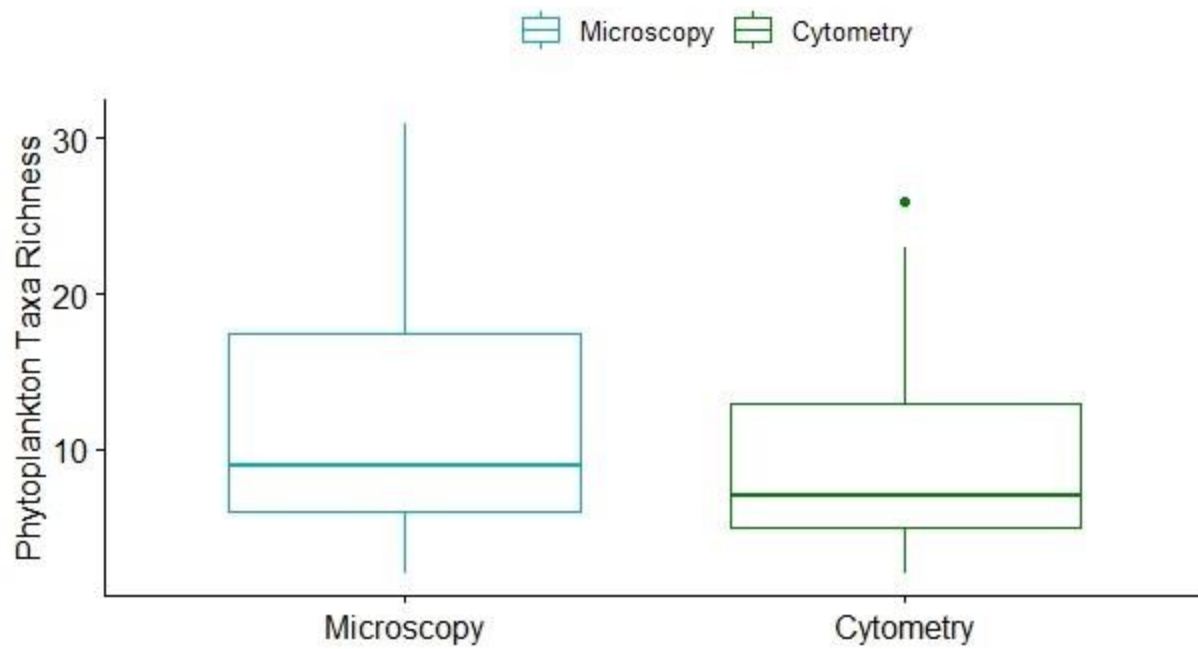


Figure 7: Boxplot showing overall phytoplankton taxa richness obtained by the microscopy and digital imaging flow cytometry (cytometry) methods.

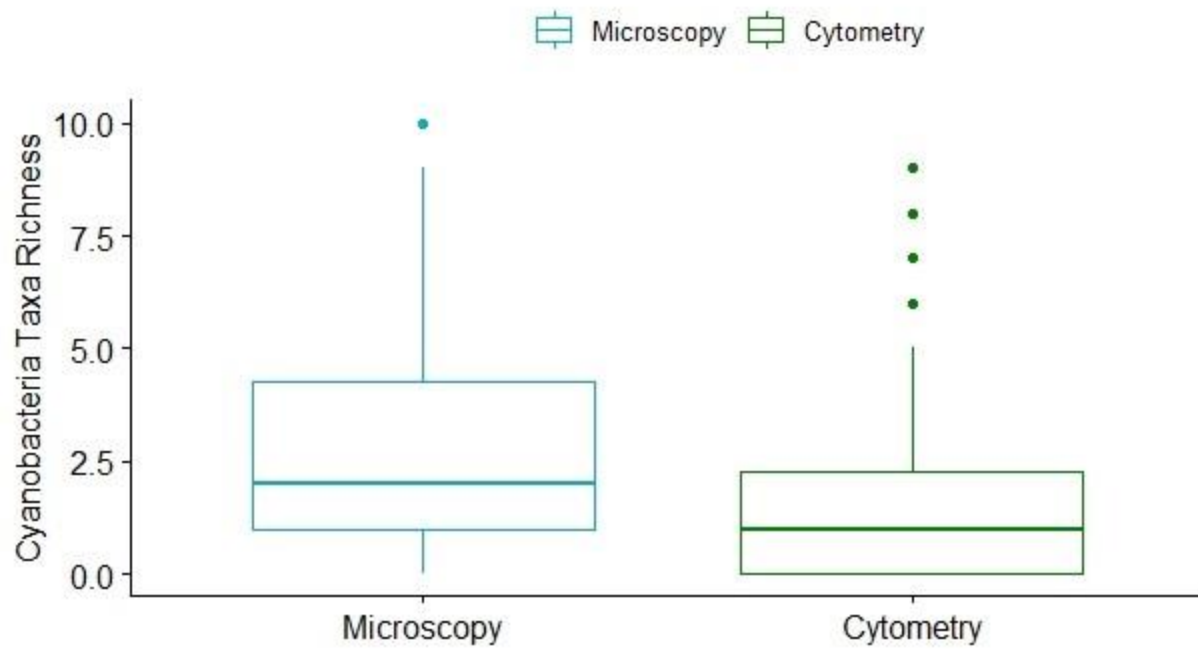


Figure 8: Boxplot showing overall cyanobacteria taxa richness obtained by the microscopy and digital imaging flow cytometry methods (cytometry).

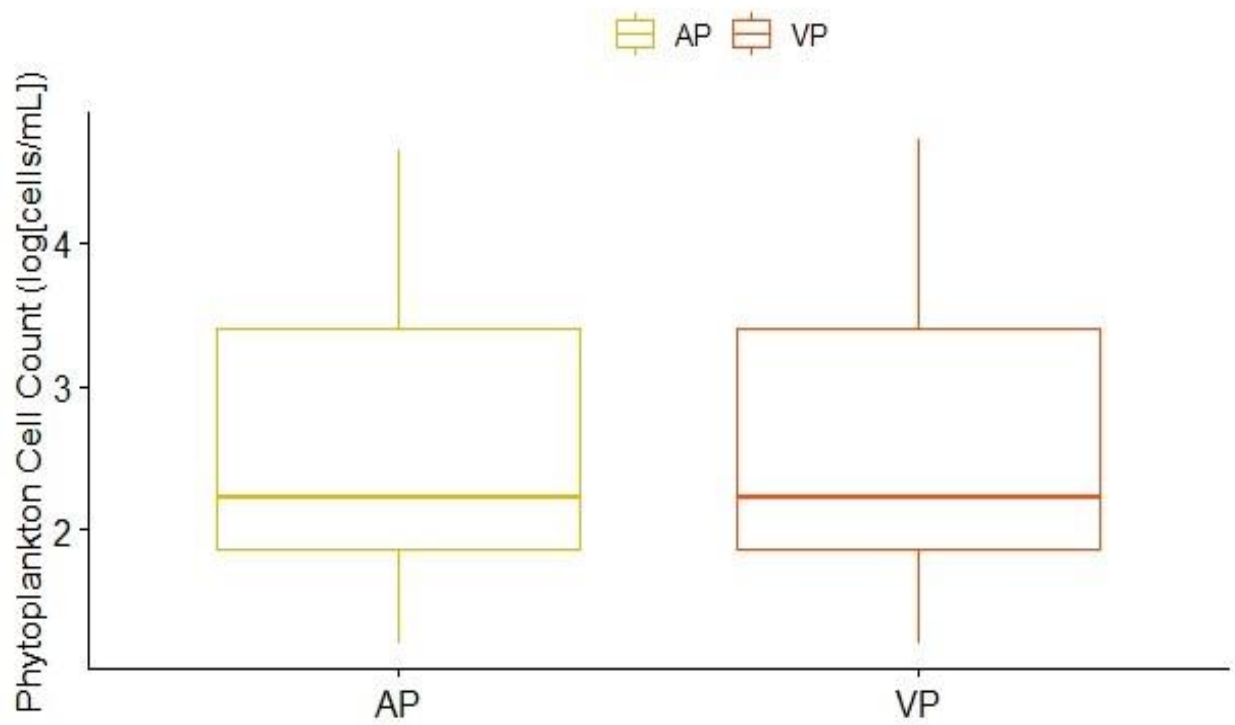


Figure 9: Boxplot showing the overall phytoplankton cell densities (cells/mL) obtained by the digital imaging flow cytometry's AP and VP attributes, plotted on a logarithmic scale.

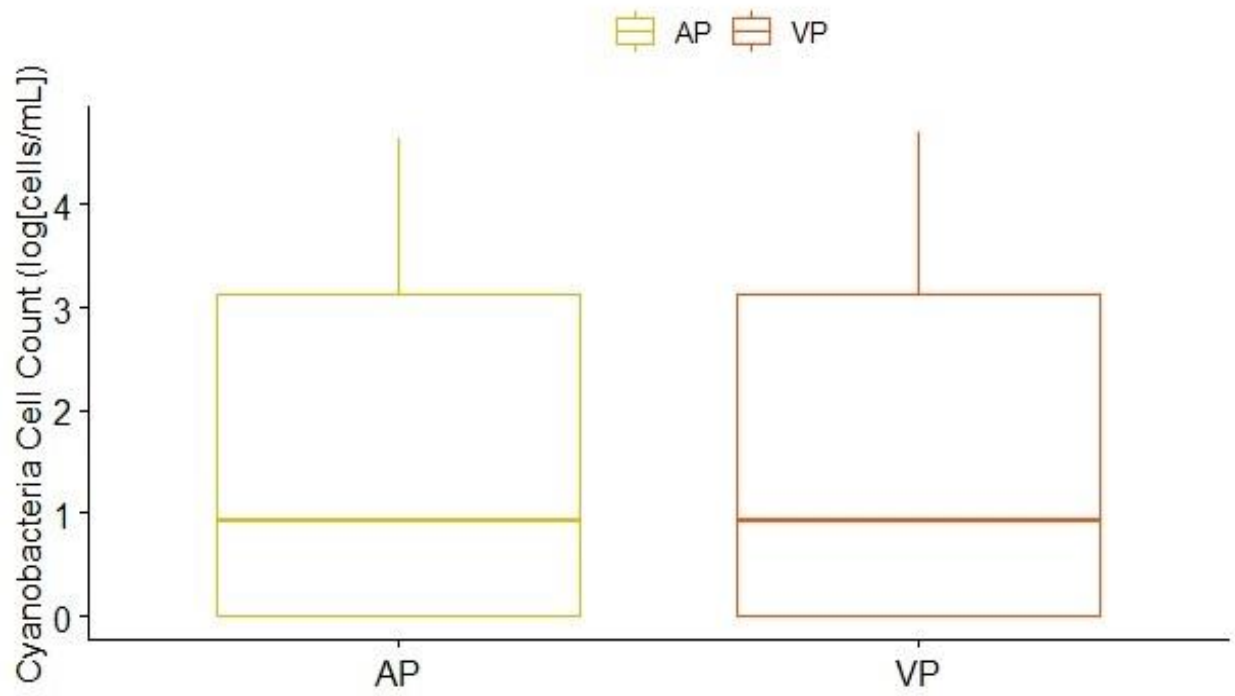


Figure 10: Boxplot showing the overall cyanobacteria cell densities (cells/mL) obtained by the digital imaging flow cytometry's AP and VP attributes, plotted on a logarithmic scale.

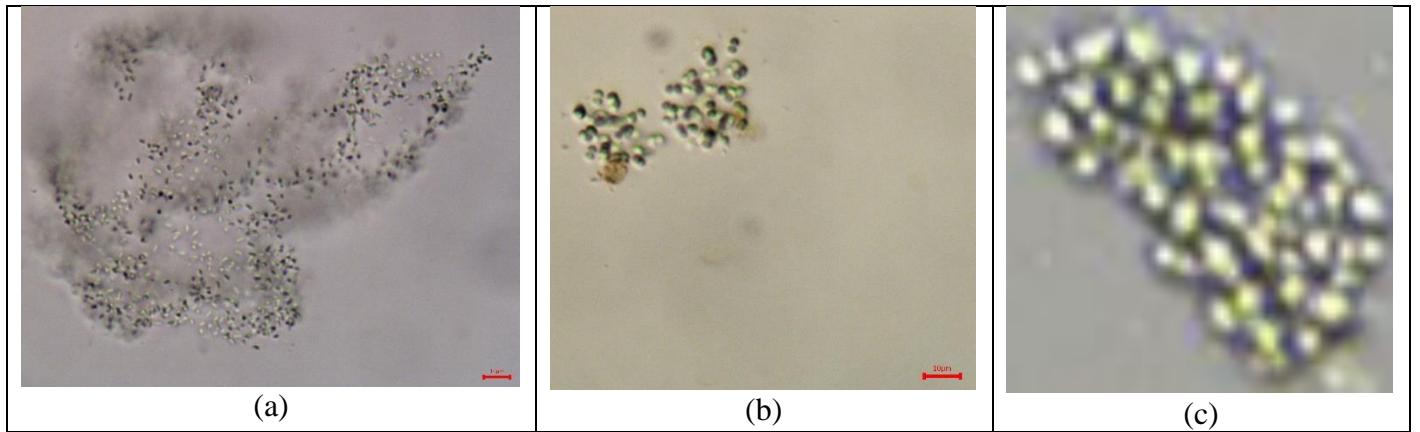


Figure 11. Images of *Aphanothece* and images of *Aphanocapsa*. (a): a compound light microscope image of an *Aphanothece* colony taken under 400X total magnification, displaying its rod-shaped cells that are similar to *Aphanocapsa*. Scale bar is 10 μm ; (b): a compound light microscope image of an *Aphanocapsa* colony, taken under 400X total magnification. Scale bar is 10 μm ; (c): an image of an *Aphanocapsa* colony taken with the digital imaging flow cytometer, where the low image resolution makes *Aphanocapsa*'s cells less distinguishable. Photo credits: New Jersey Center for Water Science and Technology, Montclair State University.

Table 1: Location Information of the eight study sites located within the Raritan River Watershed, New Jersey.

Site ID	Location	Latitude	Longitude	Town	County
A	Budd Lake	40.862778	-74.754722	Mount Olive	Morris
B	South Branch Raritan River	40.677778	-74.879167	High Bridge	Hunterdon
C	Spruce Run Reservoir	40.64	-74.915556	Clinton	Hunterdon
D	South Branch Raritan River	40.572222	-74.868056	Stanton	Hunterdon
E	Stony Brook River	40.333952	-74.7544316	Princeton	Mercer
F	Millstone River	40.475000	-74.575833	Blackwells Mills	Somerset
G	Raritan River	40.555556	-74.582778	Manville	Somerset
H	Raritan River, below Calco Dam	40.551111	-74.548333	Bound Brook	Somerset

Table 2: Minimum, maximum, and median phytoplankton* densities (cells/ml) obtained from the microscopy and digital imaging flow cytometry method, along with the results of the pairwise comparison analysis.

Location	n	Microscopy			Digital Imaging Flow Cytometry			U Value	Pairwise Comparison Analysis
		Minimum	Maximum	Median	Minimum	Maximum	Median		
Overall:	80	310	1,085,728	4,453	16	44,378	171	1168	p < 0.001
Site A	10	92,781	1,085,728	554,535	1,234	44,378	14,771	0	p < 0.001
Site B	10	465	8,906	3,640	20	163	128	0	p < 0.001
Site C	10	20,214	106,876	56,033	3,168	16,863	8,388	0	p < 0.001
Site D	10	310	18,200	6,118	24	3,416	538	11	p < 0.001
Site E	10	465	10,843	2,401	20	769	108	3	p < 0.001
Site F	10	1,239	4,957	2,633	16	325	70	0	p < 0.001
Site G	10	387	7,280	1,472	56	529	100	1	p < 0.001
Site H	10	465	10,300	2,478	44	1,340	160	4	p < 0.001

*Cyanobacteria cell densities are included with the phytoplankton cell densities

Table 3: Minimum, maximum, and median cyanobacteria densities (cells/ml) obtained from the microscopy digital imaging flow cytometry method, along with the results of the pairwise comparison analysis.

Location	n	Microscopy			Digital Imaging Flow Cytometry			U Value	Pairwise Comparison Analysis
		Minimum	Maximum	Median	Minimum	Maximum	Median		
Overall:	80	0	1,074,641	3,369	0	42,791	9	1535.5	p < 0.001
Site A	10	42,286	1,074,641	534,269	28	42,791	13,281	1	p < 0.001
Site B	10	0	8,364	1,936	0	108	0	14	p < 0.001
Site C	10	13,631	98,899	46,506	2,732	13,765	6,834	1	p < 0.001
Site D	10	0	15,954	4,531	0	2,971	314	22	p = 0.002
Site E	10	0	6,041	1,316	0	680	0	10	p < 0.001
Site F	10	155	4,724	1,820	0	293	0	1	p < 0.001
Site G	10	0	5,731	504	0	381	0	14	p < 0.001
Site H	10	0	9,913	968	0	1,236	7	21	p = 0.003

Table 4: The minimum, maximum, and median phytoplankton* natural unit densities (NU/ml) obtained from the microscopy and digital imaging flow cytometry methods, along with the results of the pairwise comparison analysis.

Location	n	Microscopy			Digital Imaging Flow Cytometry			U Value	Pairwise Comparison Analysis
		Minimum	Maximum	Median	Minimum	Maximum	Median		
Overall:	80	310	101,089	1,394	19	1,817	108	375	p < 0.001
Site A	10	21,375	101,089	55,066	541	1,817	1,016	0	p < 0.001
Site B	10	465	2,246	1,162	20	113	66	0	p < 0.001
Site C	10	5,034	14,405	6,506	367	963	616	0	p < 0.001
Site D	10	310	3,253	1,432	24	243	100	0	p < 0.001
Site E	10	465	2,633	1,162	20	403	71	0	p < 0.001
Site F	10	697	2,478	1,046	16	285	28	0	p < 0.001
Site G	10	387	1,394	890	36	268	99	0	p < 0.001
Site H	10	387	2,866	1,123	44	312	93	0	p < 0.001

*Cyanobacteria natural unit densities are included with the phytoplankton natural unit densities.

Table 5: The minimum, maximum, and median cyanobacteria natural unit densities (NU/ml) obtained from the microscopy and digital imaging flow cytometry methods, along with the results of the pairwise comparison analysis.

Location	n	Microscopy			Digital Flow Imaging Cytometry			U Value	Pairwise Comparison Analysis
		Minimum	Maximum	Median	Minimum	Maximum	Median		
Overall:	80	0	91,306	387	0	1,330	4	1164	p < 0.001
Site A	10	2,711	91,306	39,423	4	1,330	638	0	p < 0.001
Site B	10	0	620	232	0	6	0	14	p < 0.001
Site C	10	852	8,674	2,672	164	710	314	0	p < 0.001
Site D	10	0	929	348	0	97	16	17	p = 0.001
Site E	10	0	852	310	0	8	0	7	p < 0.001
Site F	10	77	774	232	0	8	0	0	p < 0.001
Site G	10	0	620	194	0	16	0	11	p < 0.001
Site H	10	0	852	116	0	36	4	16	p = 0.001

Table 6: Minimum, maximum, and median phytoplankton* taxa richness obtained from microscopy and digital imaging flow cytometry, along with the results of the pairwise comparison analysis.

Location	n	Microscopy			Digital Imaging Flow Cytometry			U Value	Pairwise Comparison Analysis
		Minimum	Maximum	Median	Minimum	Maximum	Median		
Overall:	80	2	31	9	2	26	7	2497	p = 0.016
Site A	10	20	30	25	11	26	21	16.5	p = 0.001
Site B	10	4	11	8	2	7	7	28	p = 0.012
Site C	10	19	31	24	13	20	18	2.5	p < 0.001
Site D	10	3	17	11	3	17	8	40	p = 0.052
Site E	10	4	17	7	3	10	8	47	p = 0.094
Site F	10	4	14	7	3	7	5	16.5	p = 0.001
Site G	10	4	14	8	2	9	4	20.5	p = 0.003
Site H	10	2	12	7	5	9	7	54	p = 0.088

*Cyanobacteria taxa richness is included in the phytoplankton taxa richness.

Table 7: Minimum, maximum, and median cyanobacteria taxa richness obtained from microscopy and digital imaging flow cytometry, along with the results of the pairwise comparison analysis.

Location	n	Microscopy			Digital Flow Imaging Cytometry			U Value	Pairwise Comparison Analysis
		Minimum	Maximum	Median	Minimum	Maximum	Median		
Overall:	80	0	10	2	0	9	1	1989	p < 0.001
Site A	10	6	10	8	1	9	7	23.5	p = 0.005
Site B	10	0	3	1	0	1	0	22	p = 0.003
Site C	10	3	10	8	2	8	5	17	p = 0.002
Site D	10	0	4	3	0	5	1	38.5	p = 0.044
Site E	10	0	4	3	0	2	0	13	p < 0.001
Site F	10	1	3	2	0	2	0	9	p < 0.001
Site G	10	0	5	1	0	2	0	16	p < 0.001
Site H	10	0	3	1	0	2	1	38	p = 0.039

Table 8: The minimum, maximum, and median phytoplankton* cell densities (cells/ml) obtained by the digital imaging flow cytometry's AP and VP attributes, along with the results of the pairwise comparison analysis.

Location	n	AP			VP			U Value	Pairwise Comparison Analysis
		Minimum	Maximum	Median	Minimum	Maximum	Median		
Overall:	80	16	44,378	171	16	53,135	171	3169	p = 0.917
Site A	10	1,234	44,378	14,771	1,231	53,135	17,332	44	p = 0.075
Site B	10	20	163	128	20	163	128	50	p = 0.111
Site C	10	3,168	16,863	8,388	3,134	24,711	10,349	39	p = 0.050
Site D	10	24	3,416	538	24	3,633	540	46.5	p = 0.091
Site E	10	20	769	108	20	769	108	49.5	p = 0.111
Site F	10	16	325	70	16	325	70	50	p = 0.111
Site G	10	56	529	100	56	529	100	50	p = 0.111
Site H	10	44	1,340	160	44	1,340	160	50	p = 0.111

*Cyanobacteria cell densities are included with the phytoplankton cell densities.

Table 9: The minimum, maximum, and median cyanobacteria cell densities (cells/ml) obtained by the digital imaging flow cytometry's AP and VP attributes, along with the results of the pairwise comparison analysis.

Location	n	AP			VP			U Value	Pairwise Comparison Analysis
		Minimum	Maximum	Median	Minimum	Maximum	Median		
Overall:	80	0	42,791	9	0	51,393	9	3178	p = 0.939
Site A	10	28	42,791	13,281	28	51,393	12,570	48	p = 0.101
Site B	10	0	108	0	0	108	0	50	p = 0.111
Site C	10	2,732	13,765	6,834	2,699	23,281	8,733	39	p = 0.050
Site D	10	0	2,971	314	0	3,180	314	48	p = 0.101
Site E	10	0	680	0	0	680	0	50	p = 0.111
Site F	10	0	293	0	0	293	0	50	p = 0.111
Site G	10	0	381	0	0	381	0	50	p = 0.111
Site H	10	0	1,236	7	0	1,236	7	50	p = 0.111

References

- Álvarez, E., Moyano, M., López-Urrutia, Á., Nogueira, E., & Scharek, R. (2014). Routine determination of plankton community composition and size structure: a comparison between FlowCAM and light microscopy. *Journal of plankton research*, 36(1), 170-184.
- Buskey, E. J., & Hyatt, C. J. (2006). Use of the FlowCAM for semi-automated recognition and enumeration of red tide cells (*Karenia brevis*) in natural plankton samples. *Harmful Algae*, 5(6), 685-692.
- Camoying, M. G., & Yñiguez, A. T. (2016). FlowCAM optimization: Attaining good quality images for higher taxonomic classification resolution of natural phytoplankton samples. *Limnology and Oceanography: Methods*, 14(5), 305-314.
- Carey, C. C., Ibelings, B. W., Hoffmann, E. P., Hamilton, D. P., & Brookes, J. D. (2012). Eco-physiological adaptations that favour freshwater cyanobacteria in a changing climate. *Water research*, 46(5), 1394-1407.
- Chapra, S. C., Boehlert, B., Fant, C., Bierman Jr, V. J., Henderson, J., Mills, D., ... & Paerl, H. W. (2017). Climate change impacts on harmful algal blooms in US freshwaters: a screening-level assessment. *Environmental Science & Technology*, 51(16), 8933-8943.
- Chorus, I. & Welker, M. (2021). *Toxic Cyanobacteria in Water: A Guide to Their Public Health Consequences, Monitoring and Management: Vol. Second edition*. CRC Press.
- Cox, P. A., Banack, S. A., & Murch, S. J. (2003). Biomagnification of cyanobacterial neurotoxins and neurodegenerative disease among the Chamorro people of Guam. *Proceedings of the National Academy of Sciences*, 100(23), 13380-13383.
- Cui, J., Jin, Z., Wang, Y., Gao, S., Fu, Z., Yang, Y., & Wang, Y. (2021). Mechanism of eutrophication process during algal decomposition at the water/sediment interface. *Journal of Cleaner Production*, 309, 127175.
- Ferrão-Filho, A. D. S., & Kozlowsky-Suzuki, B. (2011). Cyanotoxins: bioaccumulation and effects on aquatic animals. *Marine drugs*, 9(12), 2729-2772.
- Fluid Imaging Technologies. (2017). *FlowCam Series Dynamic Imaging Particle Analyzer User Guide*. Fluid Imaging Technologies, Inc. <https://www.kenelec.com.au/wp-content/uploads/2018/08/FlowCam-8000-Series-UserGuide.pdf>
- Griffith, A. W., & Gobler, C. J. (2020). Harmful algal blooms: a climate change co-stressor in marine and freshwater ecosystems. *Harmful Algae*, 91, 101590.
- Hällfors, G., Melvasalo, T., Niemi, Å. and Viljamaa, H. (1979) Effect of different fixatives and preservatives on phytoplankton counts. *Publications of the Water Research Institute* 34, 25-34.

- Ho, J. C., Michalak, A. M., & Pahlevan, N. (2019). Widespread global increase in intense lake phytoplankton blooms since the 1980s. *Nature*, 574(7780), 667-670.
- Hrycik, A. R., Shambaugh, A., & Stockwell, J. D. (2019). Comparison of FlowCAM and microscope biovolume measurements for a diverse freshwater phytoplankton community. *Journal of Plankton Research*, 41(6), 849-864.
- Jin, C., Mesquita, M. M., Deglint, J. L., Emelko, M. B., & Wong, A. (2018). Quantification of cyanobacterial cells via a novel imaging-driven technique with an integrated fluorescence signature. *Scientific reports*, 8(1), 1-12.
- Kidwell, DM. (2015). *Programmatic Environmental Assessment for The Prevention, Control, And Mitigation of Harmful Algal Blooms Program*. National Oceanic and Atmospheric Administration https://cdn.coastalscience.noaa.gov/page-attachments/about/pcm_hab_pea_finaldoc.pdf
- Komárek, J. & Anagnostidis, K. (2008). Cyanoprokaryota-1. Teil/Part 1: Chroococcales. In H. Ettl, G. Gärtner, H. Heynig, & D. Mollenhauer (Eds.), *Süßwasserflora von Mitteleuropa* (Vol. 19/1, pp. xyz). Heidelberg, Germany: Spektrum.
- Komárek, J. & Anagnostidis, K. (2008). Cyanoprokaryota-2. Teil/Part 2: Oscillatoriales. In B. Büdel, G. Gärtner, L. Krienitz, & M. Schagerl (Eds.), *Süßwasserflora von Mitteleuropa* (Vol. 19/2, pp. xyz). Heidelberg, Germany: Spektrum.
- Komárek, J. (2013). Cyanoprokaryota-3. Teil/Part 3: Heterocytous Genera (J. R. Johansen, Ed.). In B. Büdel, G. Gärtner, L. Krienitz, & M. Schagerl (Eds.), *Süßwasserflora von Mitteleuropa* (Vol. 19/3, pp. xyz). Heidelberg, Germany: Springer Spektrum.
- Liu, H., Song, X., Huang, L., Zhong, Y., Shen, P., & Qin, G. (2011). Diurnal variation of phytoplankton community in a high frequency area of HABs: Daya Bay, China. *Chinese Journal of Oceanology and Limnology*, 29(4), 800-806.
- Lehman, P. W., Kurobe, T., Lesmeister, S., Baxa, D., Tung, A., & Teh, S. J. (2017). Impacts of the 2014 severe drought on the *Microcystis* bloom in San Francisco Estuary. *Harmful Algae*, 63, 94-108.
- Menden-Deuer, S., Lessard, E. J., & Satterberg, J. (2001). Effect of preservation on dinoflagellate and diatom cell volume and consequences for carbon biomass predictions. *Marine Ecology Progress Series*, 222, 41-50.
- Metcalf J.S., Codd G.A. (2012) Cyanotoxins. In: Whitton B. (eds.) *Ecology of Cyanobacteria II*. Springer, Dordrecht. https://doi.org/10.1007/978-94-007-3855-3_24
- Mullin, M. M. (2001). Plankton. In J. K. Cochran, H. J. Bokuniewicz, P. L. Yager (eds.), *Encyclopedia of ocean sciences* (3rd ed.), (pp. 613-614). Academic Press.
- New Jersey Department of Environmental Protection. (2021). *2021 Cyanobacterial Harmful Algal Bloom (HAB) Freshwater Recreational Response Strategy*. NJ Department of Environmental Protection, Division of Water Monitoring and Standards, Bureau of

Freshwater & Biological Monitoring.

https://www.state.nj.us/dep/hab/download/HAB2021StrategyFinal.pdf?utm_medium=email&utm_source=govdelivery

- Olsen, P. S., & Mahoney, J. B. (2001). Phytoplankton in the Barnegat Bay—Little Egg Harbor estuarine system: Species composition and picoplankton bloom development. *Journal of Coastal Research*, 115-143.
- Park, J., Kim, Y., Kim, M., & Lee, W. H. (2019). A novel method for cell counting of *Microcystis* colonies in water resources using a digital imaging flow cytometer and microscope. *Environmental Engineering Research*, 24(3), 397-403.
- Piontkovski, S. A., Al-Gheilani, H. M. H., Jupp, B., Sarma, Y. V. B., & Al-Azri, A. R. (2012). The relationship between algal blooms, fish kill incidents, and oxygen depletions along the Omani coast. *International Journal of Oceans and Oceanography*, 6(2), 145-177.
- Rabalais, N. N., Turner, R. E., & Wiseman Jr, W. J. (2002). Gulf of Mexico hypoxia, aka “The dead zone”. *Annual Review of ecology and Systematics*, 33(1), 235-263.
- Shan, K., Song, L., Chen, W., Li, L., Liu, L., Wu, Y., ... & Peng, L. (2019). Analysis of environmental drivers influencing interspecific variations and associations among bloom-forming cyanobacteria in large, shallow eutrophic lakes. *Harmful algae*, 84, 84-94.
- Sieracki, C. K., Sieracki, M. E., & Yentsch, C. S. (1998). An imaging-in-flow system for automated analysis of marine microplankton. *Marine Ecology Progress Series*, 168, 285-296.
- Wehr, J. D., Sheath, R. G., & Kociolek, J. P. (2015). *Freshwater algae of North America: ecology and classification* (2nd ed.). London: Elsevier Academic Press.
- Yokogawa Fluid Imaging Technologies. (2020). *Visual Spreadsheet 5 FlowCam Image Analysis Software User Guide, Appendices, and Particle Properties Definitions*. Fluid Imaging Technologies, Inc.
- Yokogawa Fluid Imaging Technologies. (n.d). *Cell Enumeration of Colonial and Filamentous Cyanobacteria with FlowCam: Method & Case Study*. Fluid Imaging Technologies, Inc. https://info.fluidimaging.com/hubfs/documents/Tech_Briefs/Colonial%20Cell%20Enumeration%20and%20Filamentous%20Cyanobacteria%20Tech%20Note.pdf?hsLang=en
- Yokogawa Fluid Imaging Technologies. (2018). *FlowCam Imaging Particle Analysis System: Identify & Classify Aquatic Microorganisms*. Yokogawa Fluid Imaging Technologies, Inc. <https://info.fluidimaging.com/hubfs/FlowCam%208000%20Aquatic%20General.pdf>